

# Iodine as a Visible Probe for the Evaluation of Zeolite Donor Strength

S. Y. Choi,<sup>†</sup> Y. S. Park,<sup>†</sup> S. B. Hong,<sup>‡</sup> and K. B. Yoon<sup>\*,†</sup>

Contribution from the Department of Chemistry, Sogang University, Seoul 121-742, Korea, and Korea Institute of Science and Technology, Seoul 130-650, Korea

Received June 27, 1996<sup>⊗</sup>

**Abstract:** The visible absorption band of iodine adsorbed on zeolite blue-shifted with increasing the electropositivity of the counteranion and the aluminum content in the framework. This phenomenon was attributed to the increase in the donor strength of the zeolite framework based on the analogous spectral shift of iodine in solution. In support of this, a negative linear correlation was observed between the measured visible bands of iodine adsorbed on various zeolites and their calculated Sanderson's intermediate electronegativities. However, the simultaneous change in the electrostatic field strength within the zeolite pores, as a result of the change in the number and the size of the cation, has to be taken into account in order to interpret the overall spectral shifts more precisely. The iodine band sensitively blue-shifted with decreasing the moisture content in the framework but red-shifted with the loss of NH<sub>3</sub> from NH<sub>4</sub><sup>+</sup>-exchanged zeolites. The visible band of iodine also progressively red-shifted with increasing the adsorbed amount, presumably due to the nature of iodine to deplete electron density from the framework. The framework structure also affected the spectral shift of the visible iodine band. The overall results established that iodine can be used as a novel molecular probe for the quantitative evaluation of the zeolite donor strength.

## Introduction

The donor–acceptor interaction between various molecules or substances is one of the most fundamental processes in chemistry.<sup>1–5</sup> However, it needs to be underlined that there are no absolute donors (D) or acceptors (A). Hence, any molecule or substance can play the role of either a donor or an acceptor just depending on the electronic nature of the interacting counterparts.

The same principle can be extended to zeolite which is a class of three-dimensionally interconnected inorganic polymers consisting of silicon, aluminum, and oxygen atoms, along with the exchangeable charge-balancing cations, which exist within the voids created by the negatively charged framework. It is therefore reasonable to expect that either the framework or the counteranion, individually or in combination, would exert a donor<sup>6–9</sup> or an acceptor<sup>10–18</sup> property toward the incorporated guest molecules depending on their relative electron richness.<sup>19</sup>

Indeed, such an amphoteric behavior of zeolite has been demonstrated during the catalytic reactions over zeolites.<sup>20–27</sup> Typically, the reaction of toluene with methanol over LiY led to the exclusive formation of the ring-alkylated products (xylene mixtures), whereas the reaction over CsX resulted in the exclusive formation of the side-chain alkylated products, i.e., ethylbenzene and styrene.<sup>26</sup> Thus, it is evident that LiY acted as a typical acid catalyst, while CsX behaved as a base catalyst. Likewise, zeolites have shown highly distinctive behaviors of either electron acceptors (acids) or donors (bases), depending on the nature of the cation, the Si/Al ratio, and other modifications. Accordingly, a large number of experimental<sup>28–48</sup> and

<sup>†</sup> Sogang University.

<sup>‡</sup> Korea Institute of Science and Technology.

<sup>⊗</sup> Abstract published in *Advance ACS Abstracts*, September 15, 1996.

(1) Mulliken, R. S.; Person, W. B. *Molecular Complexes: A Lecture and Reprint Volume*; Wiley: New York, 1969.

(2) Kosower, E. M. *Adv. Phys. Org. Chem.* **1965**, *3*, 81.

(3) Davidson, R. S. In *Molecular Association*; Foster, R., Ed.; Academic: New York, 1975; Vol. 1.

(4) Davidson, R. S. *Adv. Phys. Org. Chem.* **1983**, *19*, 1.

(5) Kochi, J. K. *Acta Chem. Scand.* **1990**, *44*, 409.

(6) Flockhart, B. D.; McLoughlin, L.; Pink, R. C. *J. Catal.* **1972**, *25*, 305.

(7) Flockhart, B. D.; Megarry, M. C.; Pink, R. C. In *Molecular Sieves*; Meier, W. M., Uytterhoeven, J. B., Eds.; Adv. Chem. Ser. 121; American Chemical Society: Washington, DC, 1973; p 509.

(8) Turkevich, J.; Ono, Y. *Adv. Catal.* **1969**, *20*, 135.

(9) Khulbe, K. C.; Mann, R. S.; Manooogian, A. *Zeolites* **1983**, *3*, 360.

(10) Stamires, D. N.; Turkevich, J. *J. Am. Chem. Soc.* **1964**, *86*, 749.

(11) Dollish, F. R.; Hall, W. K. *J. Phys. Chem.* **1967**, *71*, 1005.

(12) Ramamurthy, V.; Caspar, J. V.; Corbin, D. R. *J. Am. Chem. Soc.* **1991**, *113*, 594.

(13) Caspar, J. V.; Ramamurthy, V.; Corbin, D. R. *J. Am. Chem. Soc.* **1991**, *113*, 600.

(14) (a) Xu, T.; Haw, J. F. *J. Am. Chem. Soc.* **1994**, *116*, 10188, (b) 7753. (c) Werst, D. W.; Tartakovsky, E. E.; Piosos, E. A.; Trifunac, A. D. *J. Phys. Chem.* **1994**, *98*, 10249.

(15) Cano, M. L.; Corma, A.; Fornés, V. García, H. *J. Phys. Chem.* **1995**, *99*, 4241.

(16) Liu, X.; Iu, K.-K.; Thomas, J. K.; He, H.; Klinowski, J. *J. Am. Chem. Soc.* **1994**, *116*, 11811.

(17) Chen, F. R.; Fripiat, J. J. *J. Phys. Chem.* **1992**, *96*, 819.

(18) Zhdanov, S. P.; Kotov, E. I. In *Molecular Sieves*; Meier, W. M., Uytterhoeven, J. B., Eds.; Adv. Chem. Ser. 121; American Chemical Society: Washington, DC, 1973; p 240.

(19) Yoon, K. B. *Chem. Rev.* **1993**, *93*, 321.

(20) Ono, Y. *Stud. Surf. Sci. Catal.* **1980**, *5*, 19.

(21) Kloetstra, K. R.; van Bekkum, H. *J. Chem. Soc., Chem. Commun.* **1995**, 1005.

(22) Dessau, R. M. *Zeolites* **1990**, *10*, 205.

(23) (a) Hathaway, P. E.; Davis, M. E. *J. Catal.* **1989**, *119*, 497. (b) Hathaway, P. E.; Davis, M. E. *Ibid.* **1989**, *116*, 263.

(24) Huang, M.; Kaliaguine, S. *Stud. Surf. Sci. Catal.* **1993**, *78*, 559.

(25) Yashima, T.; Sato, K.; Hayasaka, T.; Hara, N. *J. Catal.* **1972**, *26*, 303.

(26) Yashima, T.; Suzuki, H.; Hara, N. *J. Catal.* **1974**, *33*, 486.

(27) Tanabe, K.; Misono, M.; Ono, Y.; Hattori, H. *Stud. Surf. Sci. Catal.* **1989**, *51*, 1.

(28) (a) Barthomeuf, D. In *Acidity and Basicity of Solids*; Fraissard, J., Petrakis, L., Eds.; NATO ASI Series C 444; Kluwer Academic: Dordrecht, 1994; p 181. (b) Hattori, H. *Chem. Rev.* **1995**, *95*, 537. (c) Farneth, W. E.; Gorte, R. J. *Chem. Rev.* **1995**, *95*, 615.

(29) Barthomeuf, D. *Stud. Surf. Sci. Catal.* **1991**, *65*, 157.

(30) Barthomeuf, D. *J. Phys. Chem.* **1984**, *88*, 42.

(31) (a) Scokart, P. O.; Rouxhet, P. G. *J. Chem. Soc., Faraday Trans. 1* **1980**, *76*, 1476. (b) Tsuji, H.; Yagi, F.; Hattori, H. *Chem. Lett.* **1991**, 1881.

(32) Huang, M.; Kaliaguine, S. *J. Chem. Soc., Faraday Trans.* **1992**, *88*, 751.

(33) Huang, M.; Adnot, A.; Kaliaguine, S. *J. Am. Chem. Soc.* **1992**, *114*, 10005.

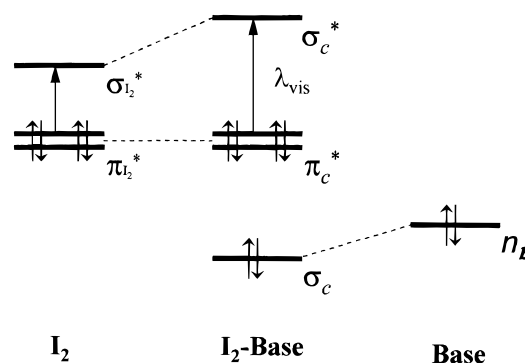
theoretical<sup>49–55</sup> studies have been directed to derive the factors that govern the donor–acceptor properties of zeolites and to develop the systematic methods to effectively monitor the properties.

The infrared studies of several probe molecules such as pyrrole,<sup>30–32</sup> benzene,<sup>35–38</sup> and carbon dioxide<sup>39–42</sup> adsorbed on zeolites have been the typical examples. Most notably, the N–H stretching band of the adsorbed pyrrole has been shown to progressively decrease with increasing the aluminum content in the framework and the electropositivity of the cation. Since pyrrole can be regarded as a weak acid,<sup>56</sup> this phenomenon was rationalized in terms of the increase in the basicity (electron-donor strength) of the oxide surfaces. Consistent with this, X-ray photoelectron spectroscopic (XPS) studies revealed a linear correlation between the decrease in the N(1s) binding energy of the adsorbed pyrrole and the decrease in the N–H stretching frequency.<sup>33,34</sup> The Sanderson's electronegativity equalization concept has been adopted as a theoretical basis, in order to account for the phenomena.<sup>28,30,32</sup>

More directly, the XPS analysis of the surface elements of zeolite has clearly demonstrated that the negative charge density on the framework oxygens indeed increases with increasing aluminum content in the framework and the electropositivity of the cation.<sup>33,43–48</sup>

As has been pointed out, however, special care should be taken in using the conventional methods. For example, the aforementioned probe molecules have been shown to be highly prone to various secondary reactions over the reactive zeolite surfaces.<sup>28,34,39–42</sup> In particular, pyrrole has been well-known to be highly vulnerable to polymerization in the presence of acidic sites.<sup>28,57,58</sup> Intrinsically, XPS analysis also has its own limits since it is mainly designed for the analysis of the external surface.<sup>45–47</sup> In this regard, it is desirable to make a continuous

Chart 1



effort to develop new experimental methods that are more viable in terms of simplicity and generality.

Stemming from our interests in the charge-transfer reactions within zeolites,<sup>19</sup> we have found that iodine can serve as a novel, alternative molecular probe for the evaluation of the zeolite donor strength. Iodine has long (more than a century) been known as a prototypical solvatochromic compound: it is violet in carbon tetrachloride as in the vapor, red in benzene, various shades of brown in alcohols and ethers, and pale yellow in water.<sup>59</sup> It has been firmly established that the dramatic color change arises primarily from the electron donor–acceptor interactions between the solvent and iodine.<sup>60–69</sup> Thus, as illustrated in Chart 1, the visible absorption of iodine corresponds to the electronic transition from  $\pi^*$  (HOMO) to  $\sigma^*$  (LUMO), where the energy level of the latter is subject to an increase in the electron-rich solvents due to the donor–acceptor interaction between iodine and the solvent.<sup>65,66,69</sup> Therefore, the higher the donor strength of the solvent, the higher the energy level of  $\sigma^*$  increases to result in the higher degree of hypsochromic shift of the visible iodine band.

Interestingly, in addition to the effect of the donor strength of the solvent on the spectral shift of the visible iodine band, our analysis has also revealed the linear relationship between the polarity of the solvent and the visible iodine band. Therefore, iodine can be regarded as a unique molecular probe to monitor for both the donor strength and the polarity of the medium.

In this paper, we report that the visible iodine band experiences dramatic spectral shifts upon adsorption on various zeolites depending on the nature of the cation, the Si/Al ratio of the framework, the dehydration temperature, and the framework structure. This phenomenon was interpreted in terms of the change in the donor strength of the framework and the

- (34) Huang, M.; Adnot, A.; Kaliaguine, S. *J. Catal.* **1992**, *137*, 322.  
 (35) Dzwigaj, S.; de Mallmann, A.; Barthomeuf, D. *J. Chem. Soc., Faraday Trans.* **1990**, *86*, 431.  
 (36) de Mallmann, A.; Barthomeuf, D. *J. Phys. Chem.* **1989**, *93*, 5636.  
 (37) de Mallmann, A.; Barthomeuf, D. *Zeolites* **1988**, *8*, 292.  
 (38) Barthomeuf, D.; Ha, B.-H. *J. Chem. Soc., Faraday Trans. 1* **1973**, *69*, 2158.  
 (39) Mirodatos, C.; Pichat, P.; Barthomeuf, D. *J. Phys. Chem.* **1976**, *80*, 1335.  
 (40) Mirodatos, C.; Abou Kais, A.; Vedrine, J. C.; Pichat, P.; Barthomeuf, D. *J. Phys. Chem.* **1976**, *80*, 2366.  
 (41) Ward, J. W.; Habgood, H. W. *J. Phys. Chem.* **1966**, *70*, 1178.  
 (42) Bertsch, L.; Habgood, H. W. *J. Phys. Chem.* **1963**, *67*, 1621.  
 (43) Barr, T. L.; Lishka, M. A. *J. Am. Chem. Soc.* **1986**, *108*, 3178.  
 (44) Okamoto, Y.; Ogawa, M.; Maezawa, A.; Imanaka, T. *J. Catal.* **1988**, *112*, 427.  
 (45) Barr, T. L. *Zeolites* **1990**, *10*, 760.  
 (46) Stoch, J.; Lercher, J.; Ceckiewicz, S. *Zeolites* **1992**, *12*, 81.  
 (47) Kaushik, V. K.; Bhat, S. G. T.; Corbin, D. R. *Zeolites* **1993**, *13*, 671.  
 (48) He, H.; Barr, T. L.; Klinowski, J. *J. Phys. Chem.* **1994**, *98*, 8124.  
 (49) Mortier, W. J. *J. Catal.* **1978**, *55*, 138.  
 (50) Mortier, W. J.; Schoonheydt, R. A. *Prog. Solid State Chem.* **1985**, *16*, 1.  
 (51) Mortier, W. J.; Ghosh, S. K.; Shankar, S. *J. Am. Chem. Soc.* **1986**, *108*, 4315.  
 (52) O'Malley, P. J.; Dwyer, J. *Chem. Phys. Lett.* **1988**, *143*, 97.  
 (53) Van Genechten, K. A.; Mortier, W. J. *Zeolites* **1988**, *8*, 273.  
 (54) Uytterhoeven, L.; Dompas, D.; Mortier, W. J. *J. Chem. Soc., Faraday Trans.* **1992**, *88*, 2753.  
 (55) Derouane, E. G.; Fripiat, J. G. *J. Phys. Chem.* **1987**, *91*, 145.  
 (56) Jones, R. A. *Adv. Heterocycl. Chem.* **1970**, *11*, 383.  
 (57) (a) Smith, G. F. *Adv. Heterocycl. Chem.* **1963**, *2*, 287. (b) Jones, R. A.; Bean, G. P. *The Chemistry of Pyrrole*; Academic: London, 1977.  
 (58) (a) Caspar, J. V.; Ramamurthy, V.; Corbin, D. R. *J. Am. Chem. Soc.* **1991**, *113*, 600. (b) Chao, T. H.; Erf, H. A. *J. Catal.* **1986**, *100*, 492.  
 (c) Bein, T.; Enzel, P. *Angew. Chem.* **1989**, *28*, 1962. (d) Roque, R.; de Onate, J.; Reguera, E.; Navarro, E. *J. Mater. Sci.* **1993**, *28*, 2321. (e) Millar, G. J.; McCann, G. F.; Hobbs, C. M.; Bowmaker, G. A.; Cooney, R. P. *J. Chem. Soc., Faraday Trans.* **1994**, *90*, 2579.

- (59) (a) Beckmann, E. Z. *Phys. Chem.* **1889**, *5*, 76. (b) Lachman, A. *J. Am. Chem. Soc.* **1903**, *25*, 50. (c) Hildebrand, J. H.; Glascock, B. L. *J. Am. Chem. Soc.* **1909**, *31*, 26. (d) Kleinberg, J.; Davidson, A. W. *Chem. Rev.* **1948**, *42*, 601.  
 (60) (a) Benesi, H. A.; Hildebrand, J. H. *J. Am. Chem. Soc.* **1948**, *70*, 2382. (b) Benesi, H. A.; Hildebrand, J. H. *J. Am. Chem. Soc.* **1949**, *71*, 2703. (c) Hildebrand, J. H. *Science* **1965**, *150*, 3695.  
 (61) Mulliken, R. S. *J. Am. Chem. Soc.* **1950**, *72*, 600.  
 (62) (a) Keefer, R. M.; Andrews, L. J. *J. Am. Chem. Soc.* **1952**, *74*, 1891. (b) Hastings, S. H.; Franklin, J. L.; Schiller, J. C.; Matsen, F. A. *J. Am. Chem. Soc.* **1953**, *75*, 2900.  
 (63) Hanna, M. W.; Lippert, J. L. In *Molecular Complexes*; Foster, R., Ed.; Else Science: London, 1973; Vol. 1.  
 (64) Mulliken, R. S. *J. Am. Chem. Soc.* **1952**, *74*, 811.  
 (65) Mulliken, R. S. *Recl. Trav. Chim. Pays-Bas* **1956**, *75*, 845.  
 (66) Nagakura, S. *J. Am. Chem. Soc.* **1958**, *80*, 520.  
 (67) Walkley, J.; Glew, D. N.; Hildebrand, J. H. *J. Chem. Phys.* **1960**, *33*, 621.  
 (68) Voigt, E. M. *J. Phys. Chem.* **1968**, *72*, 3300.  
 (69) Drago, R. S. *Physical Methods for Chemists*, 2nd ed.; Saunders College Publishing: Ft. Worth, TX, 1992; p 134.

**Table 1.** Visible Absorption Bands of Iodine Adsorbed on Na<sup>+</sup>-FAU(1.2) and K<sup>+</sup>-FAU(2.6): Effect of the Adsorbed Amount on Spectral Shift

Na <sup>+</sup> -FAU(1.2)				K <sup>+</sup> -FAU(2.6)			
I <sub>2</sub> -loading			abs	I <sub>2</sub> -loading			abs
amount <sup>a</sup>	no. <sup>b</sup>	λ <sub>max</sub> <sup>c</sup>		amount <sup>a</sup>	no. <sup>b</sup>	λ <sub>max</sub> <sup>c</sup>	
15.8	0.14	420	0.357	5.9	0.04	414	0.199
32.7	0.29	423	0.542	13.7	0.09	421	0.361
46.1	0.40	427	0.702	31.2	0.21	426	0.499
71.5	0.63	431	0.820	38.0	0.25	432	0.670
82.4	0.72	435	0.917	70.2	0.47	439	0.851
114.5	1.00	438	1.038	120.9	0.81	447	0.987

<sup>a</sup> Adsorbed amount in mg/g of zeolite. <sup>b</sup> Per Supercage. <sup>c</sup> In nanometers.

electrostatic field strength (polarity) of the zeolite surface, from the consideration of zeolites as solid solvents.<sup>70</sup>

## Results

**Effect of Adsorbed Amount.** The colorless zeolite powders with various Si/Al ratios and counterions immediately turned yellow, brown, or pink upon exposure to iodine vapor. The diffuse reflectance UV-vis spectra of the highly colored samples revealed distinct absorption maxima (λ<sub>max</sub>) in the visible region. The colors generally intensified upon increasing the adsorbed amount with the exception of small-pore zeolites such as K<sup>+</sup>-LTA<sup>71</sup> which adsorbed only limited amounts (less than 10 mg/g of zeolite).<sup>72</sup> Interestingly, upon increasing the adsorbed amount, the visible band generally red-shifted as typically demonstrated in Table 1 for Na<sup>+</sup>-FAU(1.2) and K<sup>+</sup>-FAU(2.6), where the numbers in the parentheses represent the corresponding Si/Al ratios of the frameworks.

Thus, Na<sup>+</sup>-FAU(1.2) immediately turned yellowish orange upon exposure to a small amount of iodine vapor. Although the color looked apparently the same, despite the increase in intensity, the diffuse reflectance spectroscopy revealed a progressive red-shift of the absorption maximum (λ<sub>max</sub>) from 420 to 438 nm with increasing the adsorbed amount from 15.8 to 114.5 mg/g of zeolite (from 0.14 to 1 molecule/supercage). Such a shift was more pronounced with K<sup>+</sup>-FAU(2.6). However, the degree of red-shift gradually diminished with increasing the Si/Al ratio or the electronegativity of the charge-balancing cation.

Accordingly, to study the effect of the change of the cation, the Si/Al ratio, and other factors on the visible iodine band, the adsorbed amount of iodine was maintained at about 30 mg/g of zeolite, which gave rise to an absorbance of ~0.5 (arbitrary) in the diffuse reflectance spectra, unless stated otherwise. The measured visible iodine bands (λ<sub>max</sub>) over various zeolites are listed in Table 2.

**Effect of Electropositivity of Cation.** The color of iodine adsorbed on various zeolites shifted to blue with increasing the electropositivity of the cation. For example, Li<sup>+</sup>-FAU(1.2) turned orange upon adsorption of iodine, while Na<sup>+</sup>-FAU(1.2) and K<sup>+</sup>-FAU(1.2) turned yellow-orange and pure yellow, respectively. Similarly, the developed colors of iodine over FAU(2.6) samples were pink (Li<sup>+</sup>), orange-red (Na<sup>+</sup>), and yellow-orange (K<sup>+</sup>). The related FAU(3.4) zeolites also showed the same trend of blue-shift with increasing the electropositivity

(70) Rabo, J. A.; Angell, C. L.; Kasai, P. H.; Schomaker, V. *Discuss. Faraday Soc.* **1966**, *41*, 328-349.

(71) The terms used for the zeolites used in this study were mostly taken from their structure codes since some zeolites have different names depending on the Si/Al ratio, despite their structures being identical.

(72) The limited adsorbed amounts of iodine onto K<sup>+</sup>-LTA should be attributed to the smaller pore opening of the zeolite (3 Å) than the kinetic diameter of iodine (4 Å).

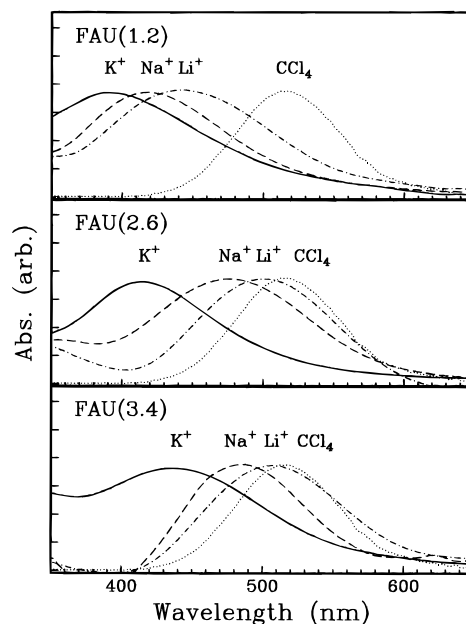


**Figure 1.** Diffuse reflectance spectra (visible region) of iodine adsorbed on a series of FAU zeolites with different cation and Si/Al ratio (as indicated). For comparison, the absorption band of iodine in CCl<sub>4</sub> is shown in the dotted line.

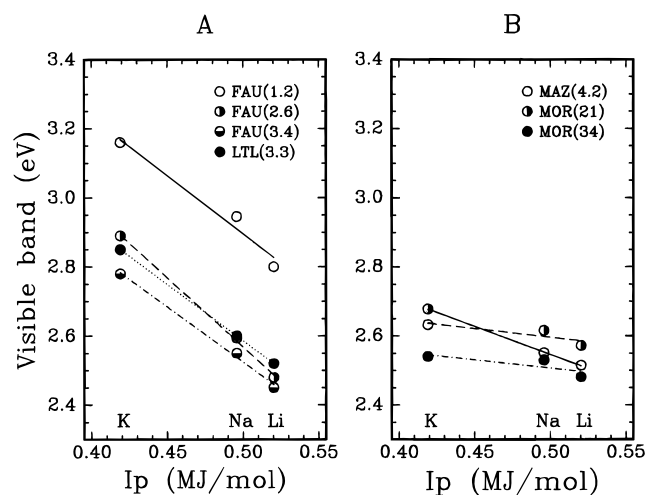


**Figure 2.** Negative linear correlations between the visible bands (in electronvolts) of iodine adsorbed on a series of alkali-metal-exchanged zeolites with different Si/Al ratios (as indicated) and the first ionization potentials ( $I_p$ ) of alkali metals as marked on the X axis.

of the cation. In accordance with the visual color change, the diffuse reflectance spectra of the colored zeolites revealed a varying degree of hypsochromic shift of the visible iodine band with changing the alkali-metal cation from Li<sup>+</sup> to Na<sup>+</sup> and to K<sup>+</sup> as illustrated in Figure 1 (compare the corresponding values of λ<sub>max</sub> in Table 2). Similar results were observed from the related series of zeolites, i.e., LTA, LTL, MAZ, and MOR.

Consistent with the above result, the plot of the visible absorption bands against the first ionization potentials ( $I_p$ ) of the three alkali-metal atoms showed excellent negative linear correlations as shown in Figure 2, regardless of the structure and the Si/Al ratio. Interestingly, the degree of the cation-induced spectral shift gradually diminished with increasing the Si/Al ratio (with decreasing the aluminum content), as judged by the much less steep or nearly flat slopes obtained from the zeolites with relatively high Si/Al ratios (Figure 2B).

In general, the visible iodine bands appeared at longer wavelengths over H<sup>+</sup>-exchanged zeolites than over the corre-

**Table 2.** Visible Absorption Band of Iodine Adsorbed on Various Zeolites<sup>a</sup> (Effect of the Cation and the Si/Al Ratio)

cation	LTA				FAU				ZSM-5					LTL	MAZ	MOR	
	Si/Al				Si/Al				Si/Al					Si/Al	Si/Al	Si/Al	
	1	1.4	2.1	2.3	1	1.2	2.6	3.4	14	28	50	150	900	3.3	4.2	21	34
K <sup>+</sup>	(421) <sup>b</sup>		(429) <sup>b</sup>	(432) <sup>b</sup>	387	393	429	446						435	463	471	488
Na <sup>+</sup>	434	448	475	485	420	421	478	486	483	501	507	511		477	486	474	490
Li <sup>+</sup>	481	483	502	502		443	501	507						493	493	482	498
H <sup>+</sup>							492		499	511	513	518	520	499	496	493	500
Ba <sup>2+</sup>							446 (435) <sup>c</sup>							495 (496) <sup>c</sup>	506 (497) <sup>c</sup>	480 (481) <sup>c</sup>	492
Sr <sup>2+</sup>							484 (466) <sup>c</sup>							493 (479) <sup>c</sup>	502 (503) <sup>c</sup>	480 (482) <sup>c</sup>	498
Ca <sup>2+</sup>							490 (495) <sup>c</sup>							490 (490) <sup>c</sup>	500 (500) <sup>c</sup>	481 (473) <sup>c</sup>	496
Mg <sup>2+</sup>							474 (496) <sup>c</sup>							490 (499) <sup>c</sup>	495 (492) <sup>c</sup>	485 (479) <sup>c</sup>	498

<sup>a</sup>  $\lambda_{\max}$  in nanometers. <sup>b</sup> Weak absorption. <sup>c</sup> Dehydrated at 500 °C.

sponding Li<sup>+</sup>-exchanged samples. Thus, as shown in Table 2, the resulting visible iodine bands ( $\lambda_{\max}$ ) invariably shifted to longer wavelengths over H<sup>+</sup>-exchanged LTL, MAZ, and MOR than over Li<sup>+</sup>-exchanged zeolites. However, in the case of FAU(2.6), H<sup>+</sup>-exchanged sample gave  $\lambda_{\max}$  at a shorter wavelength (492 nm) than that of the Li<sup>+</sup>-exchanged one (501 nm).

By contrast, the visible iodine band shifted somewhat irregularly over alkaline-earth-metal (M<sup>2+</sup>) exchanged zeolites, in particular, over the silicon-rich zeolites such as LTL, MAZ, and MOR, unlike over the zeolites exchanged with monovalent alkali-metal ions (M<sup>+</sup>). Most notably, although the increments were small, M<sup>2+</sup>-exchanged LTL and MAZ showed steady red-shifts of the visible iodine band with increasing the size of cation from Mg<sup>2+</sup> to Ba<sup>2+</sup>. Moreover, the visible iodine bands remained nearly the same over M<sup>2+</sup>-MOR samples with even higher Si/Al ratios. By contrast, the visible iodine band progressively blue-shifted in large increments over M<sup>2+</sup>-FAU(2.6) which has a relatively lower Si/Al ratio, with increasing the size of the cation, except Mg<sup>2+</sup>. However, when M<sup>2+</sup>-FAU(2.6) zeolites were dehydrated at a higher temperature (500 °C, see the Experimental Section), all the bands showed a normal trend of red-shift with increasing the electronegativity of the M<sup>2+</sup> cation (compare the values shown in the parentheses in Table 2). This result was contrasted with the persistent irregular shifts observed from the related high-silica zeolites even after dehydration at 500 °C. Thus, the visible band of iodine adsorbed on M<sup>2+</sup>-exchanged zeolites showed an interesting dichotomous behavior depending on the Si/Al ratio.

**Effect of Cation Composition.** The absorption band of iodine adsorbed on a series of zeolites exchanged with different ratios of K<sup>+</sup> and Li<sup>+</sup> gave rise to a progressive red-shift with increasing the relative amount of Li<sup>+</sup>, consistent with the aforementioned gradual red-shift of the visible iodine band with increasing the electronegativity of the cation. Thus as demonstrated in Figure 3, a dramatic red-shift from 429 to 461 nm was noticed even by 28% replacement of K<sup>+</sup> with Li<sup>+</sup> in K<sup>+</sup>-FAU(2.6). Continued increase in the Li<sup>+</sup> content by 42 and 58% yielded further red-shifts of the visible iodine band to 472 and 481 nm, respectively.

**Effect of Si/Al Ratio.** The Si/Al ratio of the zeolite framework also sensitively affected the color of iodine adsorbed on various zeolites. For example, in the case of K<sup>+</sup>-FAU zeolites, the color gradually shifted from yellow to orange with increasing the Si/Al ratio from 1.0 to 3.4. The Na<sup>+</sup>- and Li<sup>+</sup>-exchanged FAU also showed similar red-shifts with the increase in the Si/Al ratio. Typically, in the case of sodium-exchanged zeolites, the aluminum-rich zeolites (Si/Al < 4) generally turned yellow to orange upon adsorption of iodine, whereas the silicon-rich zeolites such as ZSM-5 and MOR (Si/Al > 28) turned pink or purple as the color of iodine in the vapor state or in CCl<sub>4</sub>. The zeolites with intermediate Si/Al ratios generally turned various shades of brown.

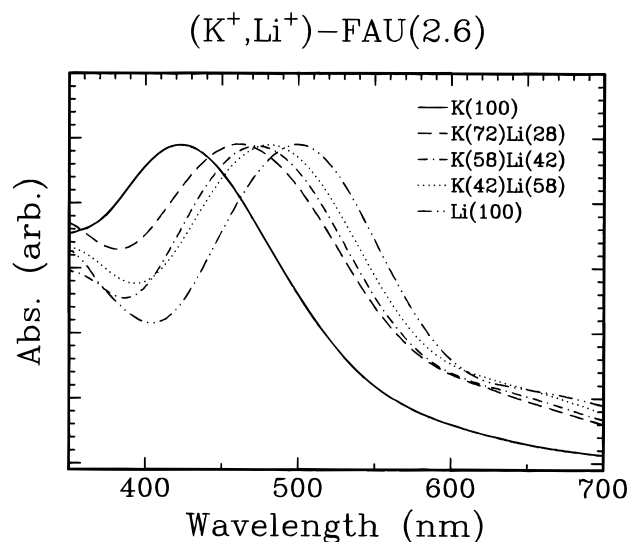


**Figure 3.** Diffuse reflectance spectra (visible region) of iodine adsorbed on a series of (K<sup>+</sup>, Li<sup>+</sup>)-FAU(2.6) zeolites exchanged with different ratios of K<sup>+</sup> and Li<sup>+</sup> (as indicated).

Consistent with the visual color change, the diffuse reflectance spectra of the colored samples demonstrated a progressive red-shift of the visible iodine band with increasing the Si/Al ratio. Thus, as already noticed from Figure 1, the visible iodine band shifted to longer wavelengths with the increase in the Si/Al ratio on going from top to bottom, for a given cation. Figure 4 further emphasizes that the degree of red-shift is larger in the aluminum-rich zeolites (top) than in the silicon-rich zeolites (bottom). Although the increments were small, the consistent red-shift of the visible iodine band with the increase in Si/Al ratio was clearly observed from Na<sup>+</sup>- and H<sup>+</sup>-exchanged ZSM-5 zeolites (see Table 2). Interestingly, the visible band ( $\lambda_{\max}$ ) of iodine adsorbed on H<sup>+</sup>-ZSM-5 with Si/Al = 900 (commonly called as silicalite) reached 520 nm as in the vapor state or in CCl<sub>4</sub>.

Consistent with the above result, Figure 5 further demonstrates good negative correlations between the measured visible iodine bands and the Si/Al ratios of some M<sup>+</sup>-exchanged FAU and LTA zeolites. Interestingly, a close examination of Figure 5 revealed that the visible iodine bands always appear at the lower energy region over Na<sup>+</sup>-LTA than over the related Na<sup>+</sup>-FAU samples throughout the entire range of the Si/Al ratio.

**Effect of Dehydration Temperature.** The visible band of iodine adsorbed on zeolite also sensitively shifted upon varying the dehydration temperature ( $T_d$ ). Interestingly, the observed patterns of the spectral shifts in response to the variation of  $T_d$  were markedly different depending on the Si/Al ratio of the framework and the type of the cation.

Typically, a gradual blue-shift of the visible iodine band was observed with increasing  $T_d$  from the zeolites exchanged with

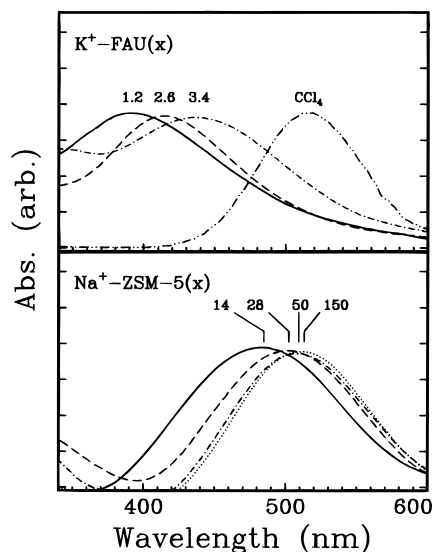


**Figure 4.** Progressive red-shift of the visible band of iodine adsorbed on  $K^+$ -FAU (top) and  $Na^+$ -ZSM-5 zeolites (bottom), with the increase in the Si/Al ratio. For comparison, the absorption band of iodine in  $CCl_4$  is included in the top figure (as indicated).

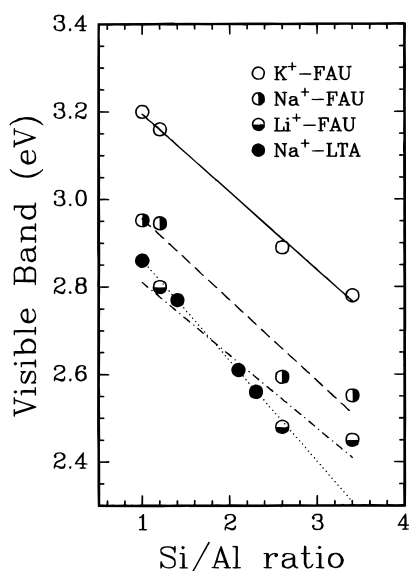


**Figure 5.** Negative linear correlations between the visible bands (in electronvolts) of iodine adsorbed on  $M^+$ -FAU ( $M = Li, Na, \text{ and } K$ ) and  $Na^+$ -LTA zeolites (as indicated) and the Si/Al ratios.

thermally stable metal ions. However, above certain dehydration temperatures, the visible iodine band usually ceased to shift and the absorption maxima reached nearly constant values. Interestingly, both the degree of blue-shift and the lowest  $T_d$  for  $\lambda_{max}$  to reach a constant value increased with increasing the aluminum content in the framework. For example, as clearly noticed in Figure 6 (left), the degree of blue-shift is more pronounced over  $Na^+$ -FAU(1.2) than over  $Na^+$ -FAU(2.6). Along with this, the lowest  $T_d$  for the visible iodine band to become invariant was 250 °C over  $Na^+$ -FAU(1.2), while the corresponding  $T_d$  was 200 °C over  $Na^+$ -FAU(2.6).

In the case of FAU zeolites exchanged with  $NH_4^+$ , which is thermally unstable, the visible iodine band also experienced a blue-shift during the initial period of water loss until  $T_d$  reached 100 °C. However, as opposed to the case of  $Na^+$ -FAU samples, the visible iodine band started to red-shift above 100 °C as  $NH_3$  began to liberate from  $NH_4^+$  ions.<sup>73</sup> The Si/Al ratio of the framework also markedly affected the pattern of the red-shift induced by  $NH_3$  loss. Thus, while  $\lambda_{max}$  of the visible band

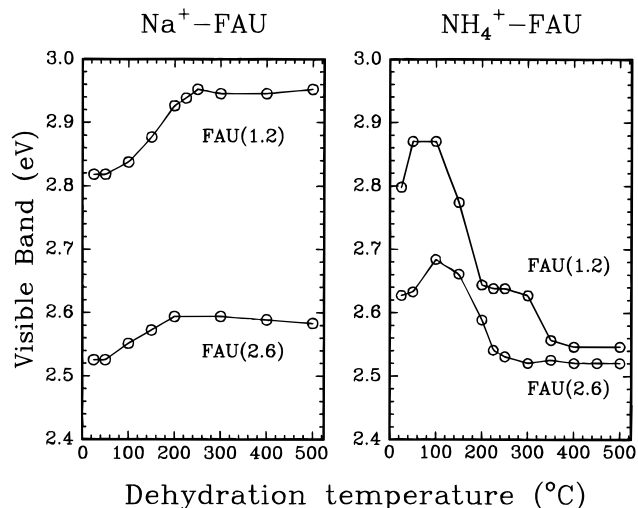


**Figure 6.** Spectral shifts of the visible band of iodine adsorbed on  $Na^+$ -FAU (left) and  $NH_4^+$ -FAU (right) with different Si/Al ratios (as indicated) as a function of the dehydration temperature ( $T_d$ ).

**Table 3.** Effect of Dehydration Temperature on the Crystallinity of  $NH_4^+$ -FAU(1.2)

$T_d$ (°C)	crystallinity (%)	$T_d$ (°C)	crystallinity (%)
100	100	300	65
150	100	400	27
200	100	500	17

became nearly constant (492 nm) at  $T_d \geq 300$  °C over  $NH_4^+$ -FAU(2.6), it became temporarily so over  $NH_4^+$ -FAU(1.2) at  $T_d$  between 200 and 300 °C, and then it suddenly shifted further to red at higher  $T_d$ . The sudden, discontinuous red-shift of the iodine band over  $NH_4^+$ -FAU(1.2) at  $T_d \geq 300$  °C was coupled with the breakage of the framework, as shown in Table 3. Thus, the analysis of each  $NH_4^+$ -FAU(1.2) sample by X-ray powder diffractometry, after dehydration at different  $T_d$ , revealed that partial breakage of the framework occurred when the samples were dehydrated at or above 300 °C, in accordance with the known instability of FAU(1.2) in the acidic form.<sup>74</sup>

## Discussion

To account for the observed spectral shifts of the visible iodine band over various zeolites, it is relevant to review the known (spectral) behavior of iodine in other media. First of all, as briefly mentioned in the Introduction, it has been well established that iodine forms electron donor-acceptor complexes with a wide variety of donor molecules, ranging from the relatively weak donors such as alkyl halides and arenes to the strong donors such as ethers, sulfides, and amines (including ammonia), both in solution<sup>60-67</sup> and in the vapor state.<sup>75-77</sup> The appearance of a new absorption band in the UV region, which is absent either from iodine or the donor upon complexation of

(73) The liberation of ammonia was confirmed by dissolving the trapped  $NH_3$  with water followed by measuring the pH of the solution.

(74) (a) Breck, D. W. *Zeolite Molecular Sieves*; Wiley: New York, 1974. (b) Barrer, R. M. *Zeolites and Clay Minerals as Sorbents and Molecular Sieves*; Academic: London, 1978.

(75) (a) Tamres, M. In *Molecular Complexes*; Foster, R., Ed.; Elke Science: London, 1973; Vol. 1. (b) Sr. Brandon, M.; Tamres, M.; Searles, S., Jr. *J. Am. Chem. Soc.* **1960**, *82*, 2129. (c) Tamres, M.; Sr. Brandon, M. *J. Am. Chem. Soc.* **1960**, *82*, 2134. (d) Evans, D. F. *J. Chem. Phys.* **1955**, *23*, 1424. (e) Lang, F. T.; Strong, R. L. *J. Am. Chem. Soc.* **1965**, *87*, 2345. (f) Ginns, E. I.; Strong, R. L. *J. Phys. Chem.* **1967**, *71*, 3059.

(76) (a) Tamres, M.; Bhat, S. N. *J. Phys. Chem.* **1971**, *75*, 1057. (b) Grundnes, J.; Tamres, M.; Bhat, S. N. *J. Phys. Chem.* **1971**, *75*, 3682. (c) Tamres, M.; Bhat, S. N. *J. Am. Chem. Soc.* **1972**, *94*, 2577.

(77) Rao, C. N. R.; Chaturvedi, G. C.; Bhat, S. N. *J. Mol. Spectrosc.* **1970**, *33*, 554.

iodine with a donor, has been successfully interpreted by the charge-transfer (CT) theory of Mulliken.<sup>64</sup>

Accordingly, the accompanying blue-shift of the visible iodine band upon CT complexation of iodine with a donor has been interpreted in terms of the perturbation of the iodine LUMO ( $\sigma^*$ ) by the donor, in such a scheme as depicted in Chart 1.<sup>65,66,69</sup> The theory has accorded well with the observed trend of the visible iodine band, i.e., the donor-strength-dependent blue-shift, both in solution and in the vapor state.

This formulation, however, was once questioned based on the failure,<sup>68,78</sup> due to experimental difficulties, to observe the blue-shifted iodine bands in the vapor state even after complexation with the relatively strong donors such as ethers and sulfides. However, the theory was soon reassured by finding the presence of the blue-shifted visible iodine bands from the above systems under more favorable conditions.<sup>76</sup> In this regard, although there are some minor discrepancies due to some secondary effects,<sup>79</sup> the spectral shift of the visible iodine band established in various solutions primarily bears a direct relationship with the change in the donor strengths of the solvents.

Second, although the effect of the solvent polarity on the spectral shift has been underestimated, our analysis revealed a general trend<sup>80</sup> of hypsochromic shift of the visible iodine band with the increase in the polarity (dielectric constant) of the solvent, consistent with the reported blue-shift with increasing the concentration of amines due to the increase in the overall polarity of the solution.<sup>68</sup> Although there is no theoretical explanation as yet to account for the polarity-dependent blue-shift of the visible iodine band, it can be attributed to the interaction of the large quadrupole and induced dipole moments of iodine with the electrostatic field of the solvent cage.

Therefore, on the basis of the above two facts, it has now become clear that the increase in the donor strength and/or the polarity of the solvent leads to a blue-shift of the visible iodine band. Accordingly, we attempted to interpret the observed spectral shifts over zeolites in terms of the change in the donor strength of the framework and/or the electrostatic field strength (polarity) of the zeolite surface, since zeolites are akin to solid electrolytic solvents.<sup>70</sup> In particular, the attempt to interpret the spectral shifts in terms of the latter is also pertinent, since the electrostatic field strengths in zeolites have been known to be extremely high and estimated to be in the order of  $10^{10}$  V m<sup>-1</sup> in the vicinity of the cations.<sup>70,81-84</sup> Such extremely high electrostatic fields have even rendered the forbidden vibrational transitions of O<sub>2</sub>,<sup>82,85</sup> N<sub>2</sub>,<sup>83</sup> and CH<sub>4</sub><sup>86,87</sup> to occur, upon adsorption of the molecules onto the cations, due to induced polarization.

**Effect of Cation.** On the basis of the above discussion, the progressive blue shift of the visible iodine band in Figure 1 upon changing the cation from Li<sup>+</sup> to Na<sup>+</sup> and to K<sup>+</sup> should be related to the increase in the donor strength and/or the electrostatic field strength of the framework surface. However, despite the presence of strong electrostatic fields in the vicinity of the cations, the interpretation of the above result in terms of

the increase in the electrostatic field is not pertinent because of the reasons stated below.

Most of all, the electrostatic field strengths in the vicinity of the cation has been proposed to decrease with increasing the size of the cation.<sup>70,74,84,88,89</sup> Therefore, we would rather expect the opposite direction of the shift (red-shift) on going from Li<sup>+</sup> to Na<sup>+</sup> and to K<sup>+</sup>. Furthermore, the X-ray crystallographic analysis of the iodine adsorbed on Ca<sup>2+</sup>-LTA by Seff and Shoemaker<sup>90</sup> revealed that the sites of iodine adsorption are not the cations but the framework oxygens, in particular those that are placed away from the cations, hence the most negatively charged. Barrer and Wasilewski<sup>91</sup> also concluded similarly based on the analysis of the isosteric heat of adsorption of iodine over several zeolites, despite the large quadrupole and induced-dipole moments of iodine. Therefore, on the basis of the fact that iodine preferentially adsorbs on the framework oxygens remote to the cations, it is expected that the variation of the electrostatic field strengths exerted on the adsorbed iodine, due to the change of cations, is rather indirect or minor.

Accordingly, the progressive blue-shift of the visible iodine band in response to the change of the cation from Li<sup>+</sup> to Na<sup>+</sup> and to K<sup>+</sup> should primarily be attributed to the progressive increase in the donor strength of the framework, consistent with the results obtained by others.<sup>28,33,50</sup> Thus, we propose that the effect of the change in the framework donor strength, as a result of the change in the size of the cation, is more important than the change in the electrostatic field strength on governing the spectral shifts of the visible iodine band.

Furthermore, the consistent blue-shifts observed from the other zeolites exchanged with alkali-metal ions (M<sup>+</sup>) in Table 2 suggest that this conclusion is general regardless of the framework structure and the Si/Al ratio. By the same analogy, the progressive red-shift of the visible iodine band in Figure 3 upon increasing the relative amount of the more electronegative cation (Li<sup>+</sup>) in the mixed cationic zeolites is attributed to the decrease in the donor strength of the zeolite framework.

However, some minor discrepancies were observed from the zeolites exchanged with alkaline-earth-metal ions (M<sup>2+</sup>), in particular, from those with high Si/Al ratios (LTL, MAZ, MOR). Most notably, the visible iodine band remained nearly invariant, despite the variation of the cation. Interestingly, M<sup>2+</sup>-exchanged LTL and MAZ showed small yet consistent blue-shifts with decreasing the size of the cation, in contrast to the trends observed from the corresponding M<sup>+</sup>-exchanged samples. We attribute such irregular or contrasting blue-shifts (observed from the silicon-rich M<sup>2+</sup>-exchanged zeolites) to a large, progressive increase in the electrostatic field strengths within zeolites, since the field strength is known to increase with increasing the cationic charge<sup>70,74,84,88,89</sup> and/or the Si/Al ratio.<sup>50,70,74,84</sup>

Nevertheless, the general appearance of the visible iodine band at longer wavelengths over M<sup>2+</sup>-exchanged LTL, MAZ, and MOR than over the corresponding M<sup>+</sup>-exchanged samples,

(85) (a) Jousse, F.; Larin, A. V.; Cohen de Lara, E. *J. Phys. Chem.* **1996**, *100*, 238. (b) Soussens-Jacob, J.; Tsakiris, J.; Cohen de Lara, E. *J. Chem. Phys.* **1989**, *91*, 2649.

(86) (a) Cohen de Lara, E.; Kahn, R.; Seloudoux, R. *J. Chem. Phys.* **1985**, *83*, 2646. (b) Kahn, R.; Cohen de Lara, E.; Möller, K. D. *J. Chem. Phys.* **1985**, *83*, 2653.

(87) See also: (a) Bras, N.; Cohen de Lara, E. *J. Chem. Phys.* **1995**, *102*, 6990. (b) Delaval, Y.; Seloudoux, R.; Cohen de Lara, E. *J. Chem. Soc., Faraday Trans. 1* **1986**, *82*, 365.

(88) (a) Ward, J. W. In *Zeolite Chemistry and Catalysis*; Rabo, J. A., Ed.; ACS Monograph 171; American Chemical Society: Washington, DC, 1976; Chapter 3. (b) Ward, J. W. *J. Phys. Chem.* **1968**, *72*, 4211. (c) Ward, J. W. *J. Catal.* **1968**, *10*, 34.

(89) (a) Angell, C. L.; Schaffer, P. C. *J. Phys. Chem.* **1966**, *70*, 1413. (b) Angell, C. L. *J. Phys. Chem.* **1966**, *70*, 2420.

(90) Seff, K.; Shoemaker, D. P. *Acta Crystallogr.* **1967**, *22*, 162.

(91) Barrer, R. M.; Wasilewski, S. *Trans. Faraday Soc.* **1961**, *57*, 1140.

(78) (a) Tamres, M.; Goodenow, J. M. *J. Phys. Chem.* **1967**, *71*, 1982. (b) See also: Kroll, M. *J. Am. Chem. Soc.* **1968**, *90*, 1097.

(79) The discrepancies were observed from the solvents that form H bonding or have high dielectric constants and from the donors that have large steric hindrance.<sup>68</sup>

(80) Such a trend was observed from the solutions of alkyl halides, alcohols, and ethers, except aromatic solvents.

(81) Spackman, M. A.; Weber, H.-P. *J. Phys. Chem.* **1988**, *92*, 794.

(82) Jousse, F.; Cohen de Lara, E. *J. Phys. Chem.* **1996**, *100*, 233.

(83) Barrachin, B.; Cohen de Lara, E. *J. Chem. Soc., Faraday Trans. 2* **1986**, *82*, 1953.

(84) (a) Dempsey, E. *J. Phys. Chem.* **1969**, *73*, 3660. (b) Dempsey, E. In *Molecular Sieves*; Society of Chemical Industry: London, 1968; p 293.

despite the aforementioned pronounced blue-shift effect of the divalent cations and the large decrease in the number of cations (by one-half), is attributed to the strongly electron-withdrawing nature of the highly electronegative  $M^{2+}$  cations.

**Effect of Si/Al Ratio.** The progressive red-shifts of the visible iodine band demonstrated in Figures 1 (top to bottom), 4, and 5 can also be related to the decrease in the donor strength of the framework and/or in the electrostatic field strength, as a consequence of the increase in the Si/Al ratio. However, as mentioned earlier, the electrostatic field strengths in the vicinity of the cations have been known to increase with increasing the Si/Al ratio, due to the decrease in the framework (negative) charge density, which, in turn, diminishes the tendency of the framework to neutralize the positive charges of cations. For example, in the case of FAU zeolites, the electrostatic field strengths of the site II and site III cations have been calculated to be increasing by about 50 and 30%, respectively, with increasing the Si/Al ratio from 1 to 2. Therefore, if the change in the electrostatic field strength of the cation would govern the spectral shift of the visible iodine band, then the shift is expected to occur in the opposite direction (blue-shift).

Accordingly, the above red-shifts with the increase in the Si/Al ratio should be attributed to the decrease in the donor strength, as a result of the decrease in the aluminum content. Consistent with this, the donor strength of zeolite has been shown to be decreasing with decreasing aluminum content.<sup>28–30,32–38,43–55</sup>

The above result once more verifies that the effect of the change in the framework donor strength is more important than the change in the electrostatic field strength on governing the spectral shift of the visible iodine band, during the variation of the Si/Al ratio. As a corollary, this result also suggests that the site of iodine adsorption is not the cation but the framework oxygen, consistent with the aforementioned results of Seff et al.<sup>90</sup> and Barrer et al.<sup>91</sup>

The appearance of the visible iodine band at 520 nm on the virtually aluminum-free zeolite (Si/Al = 900) as in the vapor state (see Table 2) further supports that the negatively charged aluminums are responsible for the donor strength of the zeolite oxide surface. The highly consistent blue-shift observed from a series of  $Na^+$ -ZSM-5 zeolites with the increase in the Si/Al ratio in Figure 4 (bottom) demonstrates the remarkable consistency of the spectral shifts of the visible iodine band over a wide range of Si/Al ratio. This may be utilized to qualitatively evaluate the Si/Al ratios of zeolites of the same structure type.

The consistent red-shift of the visible iodine band over  $Na^+$ -LTA( $n$ ) with respect to the corresponding band over  $Na^+$ -FAU( $n$ ) in Figure 5, over a range of Si/Al ratios, suggests that FAU structure has intrinsically higher donor strength than LTA for a given cation and Si/Al ratio. Similarly, the appearance of the visible iodine bands at shorter wavelengths over LTL(3.3) than over FAU(3.4) in Figure 2A also suggests that LTL structure has higher donor strength than FAU for a given cation and Si/Al ratio. Thus we propose that the structure-dependent order of donor strengths is  $LTA < FAU < LTL$ .

**Relationship with the Sanderson's Intermediate Electronegativity.** In general, the change in the donor strength (basicity) of the zeolite framework, induced by varying the counter-cation and the Si/Al ratio, has been related to the change in the Sanderson's intermediate electronegativity of zeolite  $S_z$  which is expressed by

$$S_z = (S_M^p S_{Si}^q S_{Al}^r S_O^t)^{1/(p+q+r+t)} \quad (1)$$

where  $S_M$ ,  $S_{Si}$ ,  $S_{Al}$ , and  $S_O$  represent the Sanderson's electronegativities of the counter-cation, silicon, aluminum, and oxygen,

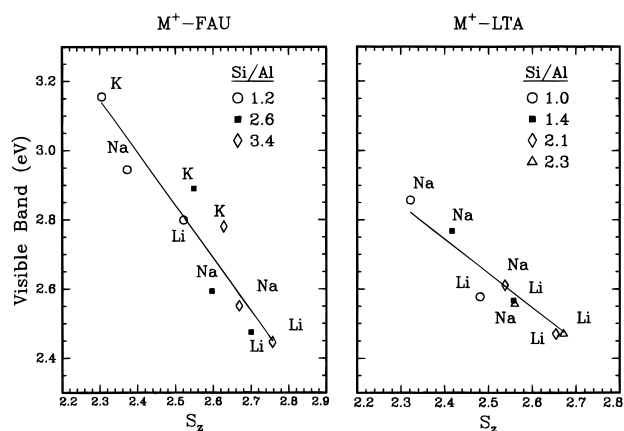


**Figure 7.** Negative linear correlations between the visible bands of iodine (in electronvolts) adsorbed on a series of alkali-metal-exchanged FAU (left) and LTA zeolites (right) with different Si/Al ratios (as indicated) and their calculated Sanderson's electronegativities.

respectively, and  $p$ ,  $q$ ,  $r$ , and  $t$  represent the number of the corresponding element, respectively, in a unit cell.<sup>28,49–51</sup> Thus, a negative linear correlation between  $S_z$  and the donor strength of the zeolite framework has been demonstrated, since the electron density on the framework oxygen (donor strength) is inversely proportional to  $S_z$ .

Consistent with the above relationship, we also found a good negative linear correlation between the calculated  $S_z$ <sup>92</sup> and the visible absorption band of iodine adsorbed on a series of  $M^+$ -exchanged FAU and LTA with different Si/Al ratios as shown in Figure 7. This result further demonstrated that the hypsochromic shifts of the visible iodine band over zeolites arise from the increase in the framework donor strength upon increasing the electropositivity of the cation and the aluminum content. As a corollary, this result indicated the donor-acceptor interaction between the adsorbed iodine and the framework oxygen, as discussed in detail later. However, the analogous plot of the visible iodine band against the calculated  $S_z$  for a series of  $M^{2+}$ -exchanged zeolites resulted in somewhat diffused negative linear correlations presumably due to the aforementioned significant change in the electrostatic field strength caused by the variation of  $M^{2+}$  ions.

**Effect of Adsorbed Amounts of Iodine.** Taking the aforementioned donor-acceptor interaction between the adsorbed iodine and the zeolite framework into account, the gradual bathochromic shift of the visible iodine band with the increase in the adsorbed amount of iodine is quite intriguing (see Table 1). Barrer and Wasilewski<sup>93</sup> also reported a similar result. Since the gradual red-shift represents the gradual decrease in the donor strength of the framework, we attribute the phenomenon to the decrease in the portion of electron density that can be donated from the framework to each of the adsorbed iodine molecules, as the adsorbed number increases, from the consideration that each zeolite microcrystal represents a large three-dimensionally linked polymeric molecule.

This interpretation is quite conceivable in view of the fact that the attachment of an electron-withdrawing group to a molecule leads to a depletion of electron density from all of the atoms within the molecule (but more pronouncingly from the neighboring atoms) by induction effects. In support of this, Barrer and Wasilewski<sup>91</sup> observed a sharp decrease in the

(92) The Sanderson's electronegativities of the elements used for the calculation of  $S_z$  were Si 2.14, Al 1.71, O 3.65, Li 0.89, Na 0.56, and K 0.45. The values were taken from: Huheey, J. E.; Keiter, E. A.; Keiter, R. L. *Inorganic Chemistry*, 4th ed.; Harper Collins College Publications: New York, 1993, pp 187ff.

(93) Barrer, R. M.; Wasilewski, S. *Trans. Faraday Soc.* **1961**, *57*, 1153.

isosteric heat of adsorption upon increasing the adsorbed amount during the initial stage of iodine occlusion (surface coverage of less than 10–20%, and the adsorbed amounts less than 100–200 mg/g of zeolite). We believe this happens because each adsorbed iodine molecule depletes some electron density from the framework (at least locally) in the same manner as do the charge-balancing cations discussed in the previous sections.

Alternatively, this phenomenon may be related to the more remotely placed average trajectories of iodine molecules from the zeolite wall, as the loading increases, assuming that iodine molecules are highly mobile and hopping around<sup>94</sup> within the pores at room temperature. This could be a possible explanation particularly when each of the zeolite cavities is filled with several iodine molecules and when iodine molecules strongly attract each other. However, from the high volatility of iodine, despite its high molecular weight, it can be deduced that the intermolecular attraction (by London force) is not so significant. Furthermore, the increase in the occupancy of the cavities with such a large molecule as iodine would decrease the mean free path of the molecule in the unadsorbed (free) state and would rather push the molecules more closely toward the zeolite wall, because of steric reasons. Therefore, it is somewhat difficult to conceive that the average trajectories of iodine would become more remotely placed by increasing the amount of loading, in particular, during the variation of loading with the maximum amount being less than one per supercage (see Table 1).

**Effect of Dehydration Temperature.** When zeolites are not fully dehydrated, the surfaces are lined by the residual polar water molecules. As a result, the direct interaction between adsorbed iodine and the negatively charged framework would be hampered by the intervening surface bound water. Accordingly, we attribute the initial blue-shifts observed from Na<sup>+</sup>-FAU samples in Figure 6 (left) with increasing  $T_d$  to the increase in the donor–acceptor interaction between iodine and the zeolite framework oxygen due to the loss of water. This may also be related to the increase in the overall electrostatic field strength of the zeolite pore as a result of the removal of water which has a high dielectric constant.

The fact that iodine bands ceased to shift upon dehydrating the samples above certain  $T_d$ , i.e.,  $\geq 200$  °C for FAU(2.6) and  $\geq 250$  °C for FAU(1.2), indicates that the framework donor strength is not further affected by higher  $T_d$  once water is completely removed. The higher degree of blue-shift observed from FAU(1.2) is ascribed to the higher donor strength of the framework in the dry state. Furthermore, the lowest  $T_d$  for visible iodine band to reach a constant wavelength being higher in FAU(1.2) ( $\geq 250$  °C) than in FAU(2.6) ( $\geq 200$  °C) is attributed to the stronger hydrophilicity of FAU(1.2) than FAU(2.6), since zeolite becomes more hydrophilic with increasing aluminum content.<sup>74</sup>

Likewise, we attribute the initial blue-shifts of the visible iodine bands over NH<sub>4</sub><sup>+</sup>-FAU samples ( $T_d \leq 100$  °C) in Figure 6 (right) to the loss of surface-lining water. However, the sudden bathochromic shifts of the visible iodine band at  $100 < T_d < 300$  °C, coupled with NH<sub>3</sub> loss, are ascribed to the generation of highly electronegative H<sup>+</sup>, as a result of the thermal decomposition of NH<sub>4</sub><sup>+</sup> ions. This is quite conceivable since the coordination of ammonia onto proton will significantly decrease the electron-withdrawing property (acidity) of proton. This result, in turn, suggests that deamination of NH<sub>4</sub><sup>+</sup>-FAU samples starts above 100 °C and becomes complete at 300 °C.

(94) The lack of free iodine bands from the highly blue-shifted visible iodine bands in Figures 1, 3, and 4 suggests that the steady-state concentration of free iodine (in the unadsorbed state) is negligible. Accordingly, the residence time of iodine on the oxygen surface is expected to be rather high.

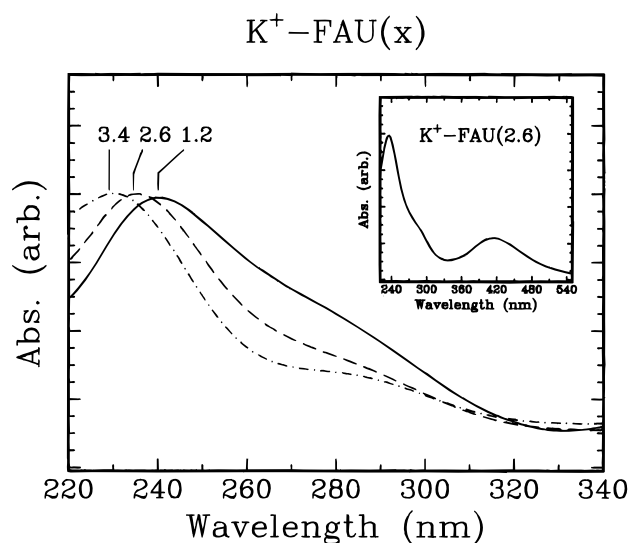


**Figure 8.** Diffuse reflectance spectra (UV region) of iodine adsorbed on a series of K<sup>+</sup>-FAU zeolites with different Si/Al ratios (as indicated). The inset shows the full-range spectrum of iodine adsorbed on K<sup>+</sup>-FAU(2.6).

The sharp red-shift observed from NH<sub>4</sub><sup>+</sup>-FAU at  $T_d > 300$  °C, coupled with the severe loss of crystallinity, suggests that iodine could also be used as a molecular probe to monitor the phase transition of zeolites.

By the same analogy, the unusual blue-shift of the visible iodine band on Mg<sup>2+</sup>-exchanged FAU(2.6) dehydrated at 300 °C (see Table 2) is attributed to the strong hydration of the cation with water due to its very high charge density,<sup>95</sup> since the coordination of a cation with water (hydration) will significantly decrease the electron-withdrawing nature of the ion as NH<sub>3</sub> does to H<sup>+</sup> in the above result.

**Nature of Interaction between Iodine and Zeolite Framework.** As discussed earlier, it has been firmly established that the blue-shift of the visible iodine band principally arises from the CT complexation between iodine and donor molecules, which also gives intense new absorption bands (CT bands) in the UV region. Accordingly, the demonstrated blue-shift of the visible iodine band over various zeolites with increasing the donor strength of the framework strongly suggests that a similar CT interaction between iodine and the oxide framework occurs. More convincingly, we also observed the appearance of new absorption bands in the UV region together with the blue-shifted visible iodine bands. In general, the newly appeared UV bands consisted of an intense band<sup>96</sup> which appears at the wavelengths ( $\lambda_{\max}$ ) shorter than 250 nm, and one or two weaker bands<sup>97</sup> which appear at wavelengths between 250 and 380 nm. As typical examples, the newly appeared UV bands obtained from the adsorption of iodine on a series of K<sup>+</sup>-FAU zeolites with different Si/Al ratios are shown in Figure 8. Interestingly, the intense, shorter wavelength band progressively red-shifted with increasing aluminum content (i.e., with increasing the donor strength of the framework). Thus, the absorption maxima progressively shifted from 230 to 235 and to 240 nm, respectively, with decreasing the Si/Al ratio from 3.4 to 2.6 and to 1.2.

(95) (a) Ward, J. W. *J. Catal.* **1968**, *11*, 251. (b) Fraissard, J.; Ito, T. *Zeolites* **1988**, *8*, 350.

(96) In general, the absorption intensity of this band was 2–3 times higher than the visible band, as typically shown in the inset of Figure 8, despite the trend of the diffuse reflectance spectroscopy which renders the absorption bands at shorter wavelengths become less pronounced.

(97) The intensities of these bands were usually weaker than those of the visible bands.



**Table 4.** Synthesis Conditions for the Zeolites Prepared in This Study

zeolites	gel composition	aging (days)	temp (°C)	time (days)
LTA(1.4)	1.5Na <sub>2</sub> O:4.1(TMA) <sub>2</sub> O:1.0Al <sub>2</sub> O <sub>3</sub> :4.0SiO <sub>2</sub> :340H <sub>2</sub> O	2	100	2
LTA(2.1)	1.45Na <sub>2</sub> O:2.05(TMA) <sub>2</sub> O:1.0Al <sub>2</sub> O <sub>3</sub> :6.0SiO <sub>2</sub> :320H <sub>2</sub> O	2	100	2
LTA(2.3)	1.45Na <sub>2</sub> O:3.05(TMA) <sub>2</sub> O:1.0Al <sub>2</sub> O <sub>3</sub> :9.0SiO <sub>2</sub> :320H <sub>2</sub> O	2	100	2.5
FAU(1.0)	5.8Na <sub>2</sub> O:1.7K <sub>2</sub> O:1.0Al <sub>2</sub> O <sub>3</sub> :2.0SiO <sub>2</sub> :130H <sub>2</sub> O	0	100	0.2
FAU(3.4)	1.0(15-crown-5):2.4Na <sub>2</sub> O:1.0Al <sub>2</sub> O <sub>3</sub> :10SiO <sub>2</sub> :140H <sub>2</sub> O	2	100	12
ZSM-5(50)	7.25Na <sub>2</sub> O:1.85(TPA) <sub>2</sub> O:0.6Al <sub>2</sub> O <sub>3</sub> :50SiO <sub>2</sub> :1800H <sub>2</sub> O	1	150	4
ZSM-5(150)	7.25Na <sub>2</sub> O:1.85(TPA) <sub>2</sub> O:0.2Al <sub>2</sub> O <sub>3</sub> :50SiO <sub>2</sub> :1800H <sub>2</sub> O	1	150	6

This band also sensitively shifted to blue with increasing the electronegativity of the cation (i.e., changing the cation from K<sup>+</sup> to Na<sup>+</sup> to Li<sup>+</sup>) and/or increasing the adsorbed amount. Consequently, the absorption maxima of the intense band could be observed only over the zeolites with high donor strengths (typically K<sup>+</sup>-exchanged zeolites with relatively low Si/Al ratios). Accordingly, the band usually showed only the tail part (longer wavelength edge) of the absorption over the zeolites with intermediate donor strengths (typically Li<sup>+</sup>-FAU) or completely disappeared from the detection limit of our instrument (220 nm) over the zeolites with poor donor strengths (typically ZSM series zeolites). In this regard, although a more extensive study is still necessary to elucidate the precise nature of the intense band as well as the insensitive weaker bands,<sup>98</sup> we tentatively assign the intense band as the CT band that arises from the CT interaction between iodine and the framework oxygens, based on the facts that the band is highly intense like the analogous iodine CT band ( $\epsilon \cong 7000-60000$ )<sup>63</sup> in solution or in the vapor state, and the band shifts sensitively in compliance with the Mulliken's CT scheme.<sup>1,64</sup>

Consistent with this, Seff and Shoemaker<sup>90</sup> revealed that the iodine molecule approaches in its axial direction to the most basic surface oxygen. The determined I...O distance was 3.29 Å, which is far less than the normal van der Waals distance (3.55 Å). The interatomic distance of iodine also significantly increased (2.79 Å) upon adsorption on the basic oxygen from its free gaseous state (2.67 Å), consistent with the theory that LUMO of iodine is  $\sigma^*$ . Therefore, we propose that the CT interaction between iodine and framework oxygens is most responsible for the ability of iodine to act as a novel probe for the zeolite donor strength.

## Experimental Section

**Materials.** LTA(1.0) (4A, Lot No. 941089060329) was purchased from Union Carbide. The related high-silica LTA(*x*) zeolites with *x* = 1.4, 2.1, and 2.3 were synthesized using mixed cations of sodium and tetramethylammonium (TMA<sup>+</sup>) according to the literature procedures.<sup>99,100</sup> FAU(1.2) (Linde 13X, Lot No. 120370) and FAU(2.6) (LZY-52, Lot No. 968087061020-S) were purchased from Strem and Union Carbide, respectively. FAU(1.0) was synthesized according to the procedure using mixed alkali of NaOH and KOH.<sup>101</sup> FAU(3.4) was synthesized using 1,4,7,10,13-pentaoxacyclopentadecane (15-crown-5) as the templating agent.<sup>102</sup> ZSM-5(*x*), *x* = 14 and 28, were the gifts from ALSI-PENTA Zeolite GmbH. ZSM-5(900) (silicalite, Lot No. 961887060021-S) was purchased from Union Carbide. ZSM-5(*x*) zeolites with *x* = 50 and 150 were synthesized using tetrapropylammonium bromide (TPA<sup>+</sup>Br<sup>-</sup>) according to the procedures.<sup>103</sup> LTL-(3.3) (ELZ-L, Lot No. 961687041001-S), MOR(21) (LZM-5, Lot No.

(98) These weaker bands showed no consistent trends of shift with the variation of the donor strengths of the framework.

(99) Kostinko, J. A. In *Intrazeolite Chemistry*; Stucky, G. D., Dwyer, F. G., Eds.; ACS Symp. Ser. 218; American Chemical Society: Washington, DC, 1983; pp 2ff.

(100) Jarman, R. H.; Melchior, M. T.; Vaughan, D. E. W. In *Intrazeolite Chemistry*; Stucky, G. D., Dwyer, F. G., Eds.; ACS Symp. Ser. 218; American Chemical Society: Washington, DC, 1983; pp 267ff.

(101) Kühl, G. H. *Zeolites* **1987**, 7, 451.

(102) Delprato, F.; Delmotte, L.; Guth, J. L.; Huve, L. *Zeolites* **1990**, 10, 546.

962487061003-S) and MOR(34) (LZM-8, Lot No. 960387061032-S) were purchased from Union Carbide. MAZ(4.2) was obtained from D. R. Corbin of the DuPont Co. The reaction conditions for the preparation of the synthesized zeolites are collected in Table 4. All the zeolites synthesized with organic structure-directing agents were calcined at 500 °C for 12 h in flowing oxygen to remove the occluded templates.

Colloidal silica (Ludox HS-40, DuPont) was used as the silicon source for the synthesis of LTA and FAU zeolites. Fumed silica (Cab-O-Sil M5, Cabot Corp.) was used for the synthesis of ZSM-5 zeolites. Sodium aluminate (Na<sub>2</sub>O·Al<sub>2</sub>O<sub>3</sub>·H<sub>2</sub>O) was purchased from Strem. TMA<sup>+</sup>OH<sup>-</sup>·5H<sub>2</sub>O and 15-crown-5 were purchased from Aldrich and TPA<sup>+</sup>Br<sup>-</sup> was purchased from Fluka. Iodine was purified by repeated sublimation.

**Ion Exchange.** Ion exchange of zeolites with monovalent cations were carried out by shaking a 1-L flask containing 1 mol of the corresponding chloride salts of Li<sup>+</sup>, Na<sup>+</sup>, K<sup>+</sup>, and NH<sub>4</sub><sup>+</sup> and 5–10 g of each zeolite at room temperature for 15 h. The bivalent-ion-exchanged zeolites were prepared by refluxing the aqueous slurries containing 5–10 g of the desired zeolites and 0.5–1 mol of the corresponding halide salts. The H<sup>+</sup>-doped zeolites were prepared from the corresponding NH<sub>4</sub><sup>+</sup>-exchanged zeolites. The ion exchanges were repeated at least five times to achieve complete exchange for the monovalent cations and maximum exchange for the bivalent cations. K<sup>+</sup>(72)Li<sup>+</sup>(28)-FAU(2.6) was prepared by stirring 10 g of K<sup>+</sup>-FAU(2.6) in 500 mL of 0.2 M LiCl solution for 15 h. K<sup>+</sup>(58)Li<sup>+</sup>(42)-FAU(2.6) was prepared similarly by stirring 7 g of K<sup>+</sup>(72)Li<sup>+</sup>(28)-FAU(2.6) in 500 mL of 0.2 M LiCl solution. Finally, K<sup>+</sup>(42)Li<sup>+</sup>(58)-FAU(2.6) was prepared by stirring 4 g of the latter in 500 mL of 0.2 M LiCl solution.

The ion-exchanged zeolites were washed with distilled deionized water (>18 MΩ) until the silver ion test for chloride was negative. The ion-exchanged samples were dried at 300 °C in vacuo (<10<sup>-5</sup> Torr) for 15 h, unless stated otherwise. The dried zeolites were then stored in a glovebox charged with high-purity argon.

**Iodine Adsorption.** Each sample (200 mg) was transferred into a flat cylindrical cell equipped with a greaseless stopcock and a joint. The cell was then removed from the glovebox and connected to an arm of an inverted-U-shaped glass tube on top of which has an access to a vacuum line through a greaseless stopcock. Independently, a glass tube containing crystalline iodine was connected to the remaining arm of the inverted-U tube. After brief evacuation of both arms in a sequential manner, the zeolite sample was allowed to adsorb iodine vapor at room temperature. The white zeolite powder turned intense yellow to purple within 10 min depending on the type of the zeolite and the cation. The coloration process greatly accelerated at elevated temperatures. The amounts of iodine adsorbed onto zeolite samples were measured by directly weighing the sample cells before and after iodine adsorption on an electronic balance.

**Instrumentation.** The diffuse reflectance UV-vis spectra of the colored samples were recorded on a Shimadzu UV-3101PC equipped with an integrating sphere. X-ray powder diffraction patterns of the synthesized zeolites were obtained from Rigaku D/MAX-1C diffractometer. To check the crystallinity of NH<sub>4</sub><sup>+</sup>-FAU(1.2), the samples were ground together with 20% of PbSO<sub>4</sub> as the internal standard. The Si/Al ratios of the synthesized zeolites as well as the commercially obtained zeolites and the K<sup>+</sup>/Li<sup>+</sup> ratios of the mixed cationic FAU zeolites were analyzed in the Analytical Laboratory of the Korea Institute of Science and Technology using a Jerrell-Ash Polyscan 61E

(103) Jacobs, P. A.; Martens, J. A. *Synthesis of High-Silica Aluminosilicate Zeolites*; Elsevier: Amsterdam, 1987.

inductively coupled plasma (ICP) spectrometer in combination with a Perkin-Elmer 5000 atomic absorption spectrophotometer. The weight of the sample containing cells were measured on a Mettler 240 electronic balance which was calibrated with standard weights.

### **Summary**

The visible band of iodine adsorbed on various zeolites sensitively shifted depending on the electropositivity of the cation, the Si/Al ratio, the dehydration temperature, and the framework structure. We attempted to interpret the observed spectral shifts in terms of the change in the donor strength of the zeolite framework and the electrostatic field strength of the zeolite pores based on the analogous shifts observed in solution. However, the results established that the effect of the change

in the donor strength of the zeolite framework is more important than the change in the electrostatic field strength on governing the spectral shifts of the visible iodine band. The CT interaction between iodine and zeolite oxide surface was proposed to be most responsible for the ability of iodine to act as a novel molecular probe for the framework donor strength of zeolite.

**Acknowledgment.** We thank the Ministry of Education (MOE), Korea, the Aided Basic Research Program of Korea Science and Engineering Foundation (KOSEF), and the Center for Molecular Catalysis (CMC) of Seoul National University, for financial support. We also thank the referees for the valuable comments and discussions.

JA952112+